Mem. S.A.It. Vol. 90, 96
© SAIt 2019

Memorie della

Broadband spectral analysis of MXB 1659-298 in its soft and hard state

S. M. Mazzola[1], R. Iaria[1], A. F. Gambino[2], A. Marino[1,3,4], T. Di Salvo[1], T. Bassi[1,3,4], A. Sanna[2], A. Riggio[2], and L. Burderi[2]

[1] Dipartimento di Fisica e Chimica - Emilio Segrè, Università degli Studi di Palermo, via Archirafi 36 - 90123 Palermo, Italy, e-mail: `simonamichela.mazzola@unipa.it`
[2] Università degli Studi di Cagliari, Dipartimento di Fisica, SP Monserrato-Sestu, KM 0.7, 09042 Monserrato, Italy
[3] INAF – Istituto di Astrofisica Spaziale e Fisica Cosmica di Palermo, Via Ugo La Malfa 153, I-90146 Palermo, Italy
[4] IRAP, Université de Toulouse, CNRS, UPS, CNES, 9 Avenue du Colonel Roche, 31400 Toulouse, France

Abstract. The X-ray transient eclipsing source MXB 1659-298 went in outburst in 1999 and 2015, respectively, during which it was observed by *XMM-Newton*, *NuSTAR* and *Swift*. Using these observations we studied the broadband spectrum of the source to constrain the continuum components and to verify the presence of a reflection component. We analysed the soft and hard state of the source, finding that the soft state can be modelled with a thermal component associated with the inner accretion disc plus a Comptonised component. A smeared reflection component and the presence of an ionised absorber are also requested in the best-fit model. On the other hand, the direct continuum emission in the hard state can be described by a Comptonised component with a temperature larger than 150 keV. Also in this case a reflection component and a ionised absorber are observed.

Key words. stars: neutron – stars: individual (MXB 1659-298) – X-rays: binaries – accretion, accretion disks

1. Introduction

MXB 1659-298 is a low mass X-ray binary (LMXB) harbouring a neutron star (NS). The source was observed in outburst three times: from 1976 up to 1978 (Cominsky et al. 1983; Cominsky & Wood 1984, 1989), from 1999 up to 2001 with *BeppoSAX*, *Rossi-XTE* and *XMM-Newton* (see e.g. in 't Zand et al. 1999; Wachter et al. 2000; Oosterbroek et al. 2001) and from 2015 up to 2017 with *Swift* (Bahramian et al. 2016) and *NuSTAR* (Sharma et al. 2018).

Studying the *XMM-Newton* spectrum of MXB 1659-298, Sidoli et al. (2001) detected two absorption lines at 6.64 and 6.90 keV associated with the presence of highly ionised iron (Fe and Fe ions) as well as absorption lines associated with highly ionised oxygen and neon. Furthermore, the authors detected the presence of a broad emission line centred at 6.47 keV and with a FWHM of 1.4 keV. Recently, Iaria et al. (2018) and Jain et al. (2017), studying the eclipse arrival times of the

Table 1. Studied observations of the source MXB 1659-298

ObsId	Instrument	Start Time (UTC)	Exposure time (ks)
0008610701	*XMM-Newton*	2001-02-20 8:28:27	31.5
0748391601	*XMM-Newton*	2015-09-26 19:53:05	42.9
90101013002	*NuSTAR*	2015-09-28 21:51:08	51.5
90201017002	*NuSTAR*	2016-04-21 14:41:08	26.8
00034002036_roll1	*Swift*	2016-04-20 01:47:54	0.67
00034002036_roll2	*Swift*	2016-04-20 01:47:54	0.13
00081918001	*Swift*	2016-04-21 20:39:01	0.70

source, suggested the presence of a third body orbiting around the binary system.

Here, we report the broadband spectral analysis of the persistent emission of MXB 1659-298 using *XMM-Newton* (including the observation studied by Sidoli et al. 2001), *NuSTAR* and *Swift*/XRT data. We analysed the spectrum of the source in soft state (SS) and hard state (HS) finding that a relativistic reflection component is necessary to describe the spectra.

2. Observations and data analysis

We were interested in the spectral analysis of the persistent emission, then we extracted the *XMM-Newton*/EPN, *XMM-Newton*/RGS and *NuSTAR* events excluding the times in which the dips, the eclipses and the type-I X-ray bursts occurred. The analysed observations are summarised in Table 1.

Analysing the RXTE/ASM and MAXI/GSC light curves of the source, we observe that the source shows a flux of 30 mCrab during the *XMM-Newton* obs. 0008610701, the *Swift* observations and the *NuSTAR* obs. 90101017002. On the other hand, the *XMM-Newton* obs. 0748391601 and the *NuSTAR* obs. 90101013002 were taken while the source flux was less than 5 mCrab. These evidences led us to fit together the persistent spectra obtained with *XMM-Newton* obs. 0748391601 and *NuSTAR* obs. 90101013002 (hereafter HS spectrum), while the persistent spectra obtained from the *XMM-Newton* obs. 0008610701, the *NuSTAR* obs. 90101017002 and the *Swift* observations are fitted together even if they were taken during two different outbursts (hereafter SS spectrum). We will show that they describe the hard and the soft state of MXB 1659-298, respectively.

The adopted energy ranges for the SS are 0.4-2 keV, 0.6-12 keV, 3-35 keV and 0.5-9 keV, for RGS12, EPN, *NuSTAR* and *Swift* spectra, respectively; while the adopted energy range for the HS are 0.45-2 keV, 0.6-12 keV and 3-55 keV for RGS12, EPN and *NuSTAR* spectra.

After fitting the SS spectrum with several models, we found that the best-fit one was composed of a disc-blackbody component (in XSPEC) plus a thermally Comptonised component (C in XSPEC, see Życki et al. 1999) to fit the continuum emission, plus a convolution component which takes into account the reflection continuum also (, see Done & Gierliński 2006; Kolehmainen et al. 2011, for details). Furthermore, we added an absorption edge with threshold energy fixed at 0.538 keV and a multiplicative component that takes into account a partial covering of ionised absorbing material (, see Reeves et al. 2008; Miller et al. 2007). We kept fixed the value of the redshift z to zero, the iron abundance to the solar one, the outer radius of the accretion disc R_{out} to 2800 gravitational radii ($R_g = GM_{NS}/c^2$) and the cosine of the inclination angle θ of MXB 1659-298 (that we assume to be 72°, Iaria et al. 2018). The other parameters were left free to vary.

For the HS spectrum, the best-fit model was the same described above without any thermal component, which resulted unnecessary to fit the spectrum. In this case, the outer radius R_{out} was kept fixed to 290 R_g.

Table 2. Best-fit parameters for the soft state and the hard state.

Model	Component	Soft State		Hard State	
		XMM-Newton	*Swift-NuSTAR*	*XMM-Newton*	*NuSTAR*
E	E (kev)	0.538 (frozen)		0.538 (frozen)	
	τ	0.24 ± 0.03		0.30 ± 0.08	
	N_H (10^22 atoms cm^{-2})	57^{+6}_{-13}		12.5 ± 1.2	
	$\log \xi_{\mathrm{IA}}$	4.36 ± 0.04	4.13 ± 0.07	2.02 ± 0.05	3.3 ± 0.3
	f	1 (frozen)		0.27 ± 0.02	
TB	N_H (10^22 atoms cm^{-2})	0.280 ± 0.013		0.31 ± 0.02	
	T_{in} (keV)	0.27 ± 0.02		-	
	$R_{\mathrm{in}} \sqrt{\cos\theta}$ (km)	50^{+5}_{-10}		-	
	Betor10	< -2.4		-2.5 ± 0.2	
	R_{in} (R_g)	39^{+35}_{-15}		< 7	
	rel_refl= $\Omega/2\pi$	0.30 ± 0.08		0.48 ± 0.06	
	$\log \xi$	$2.72^{+0.07}_{-0.10}$		$1.99^{+0.04}_{-0.11}$	
N C	Γ	1.70 ± 0.02	$2.153^{+0.019}_{-0.014}$	2.00 ± 0.02	
	kT_{e} (keV)	2.01 ± 0.04	$3.64^{+0.06}_{-0.08}$	> 150	
	kT_{bb} (kev)	0.42 ± 0.02	$0.565^{+0.018}_{-0.007}$	< 0.10	
	Norm	0.14 ± 0.02		0.0341 ± 0.0011	
	χ^2(d.o.f)	3124(2795)		2321(2269)	

We obtained a $\chi^2(d.o.f)$ of 3124(2795) and 2321(2269), respectively; we show the best-fit values in Table 2. The unfolded spectrum and the corresponding residuals are shown in Figure 1.

3. Discussion

We have analysed several spectra of MXB 1659-298 collected during the 1999 and 2015 outbursts, observing two different spectral state of the source. We find that the SS spectrum has a 0.1-100 keV unabsorbed flux of 2.2×10^{-9} erg cm^{-2} s^{-1} and it shows a soft Comptonised component with a value of the electron temperature lower than 4 keV. Furthermore, a multicolour disc component is present at low energies with an inner temperature of 0.27 keV and an inner radius of the disc $\mathrm{R_{in}} \sqrt{\cos\theta} = 50^{+5}_{-10}$ km . On the other hand, the HS spectrum shows a hard Comptonised component with a value of the electron temperature larger than 150 keV; the addition of a thermal component is not statistically significant. It is necessary to take into account a smeared reflection component to model the Fe-K region of both the spectra, where a broad emission line is observed. We find that the width of the emission line cannot be explained considering only the Compton scattering but we have to include the relativistic smearing in order to obtain a good fit. In the SS, the reflecting region of the accretion disc is between 39 and 2800 R_g and it is between 6 and 290 R_g in HS. Besides, the ionisation parameter $\log \xi$ is $2.72^{+0.07}_{-0.10}$ and $1.99^{+0.04}_{-0.11}$ in SS and HS, respectively. By analysing both the spectra we obtain that the values of the equivalent hydrogen column density are compatible with each other within 90% c.l. with a value of 0.29×10^{22} cm^{-2}. Furthermore, we observed

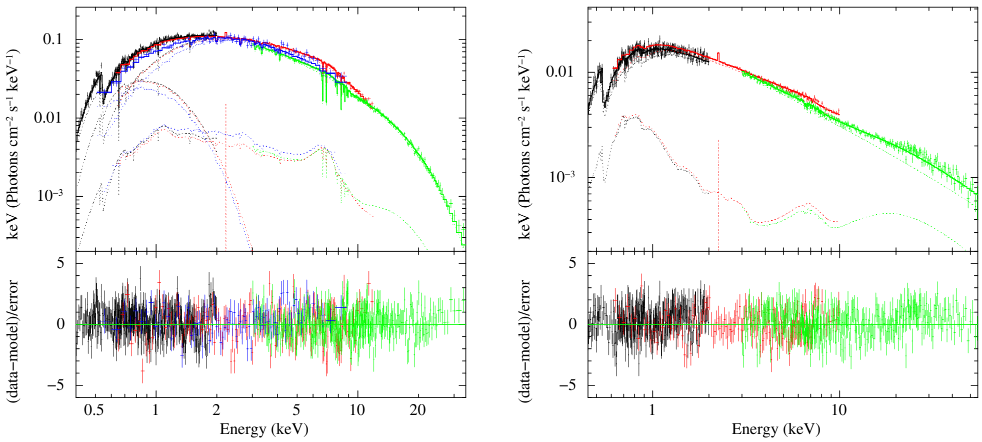

Fig. 1. Left Panel: SS spectrum and residuals corresponding to the best-fit model. The black, red, green and blue data are associated with the RGS12, EPN, *NuSTAR* and *Swift* observations, respectively. Right Panel: HS spectrum and residuals corresponding to the best-fit model. The black, red and green data are associated with the RGS12, EPN and *NuSTAR* observations, respectively.

that the source is covered by ionised absorbing matter, at least partially in the case of HS spectrum.

We estimated also the optical depth of the Comptonised cloud using the relation between the power-law photon index Γ and the electron temperature kT_e obtained by Zdziarski et al. (1996), finding that it is optically thick in the SS (i.e $8 < \tau < 16$) whilst it is optically thin in the hard state ($\tau < 0.7$).

Finally, we obtained a value of the relative reflection normalisation of 0.30 ± 0.08 in SS, compatible with a spherical corona in the inner part of the accretion disc (see Dove et al. 1997); while the value of 0.48 ± 0.06 obtained for the HS suggests a larger superposition of the corona to the disc.

Acknowledgements. We acknowledge financial contribution from the agreement ASI-INAF I/037/12/0.

References

Bahramian, A., et al. 2016, The Astronomer's Telegram, 8699
Cominsky, L., Ossmann, W., & Lewin, W. H. G. 1983, ApJ, 270, 226
Cominsky, L. R. & Wood, K. S. 1984, ApJ, 283, 765
Cominsky, L. R. & Wood, K. S. 1989, ApJ, 337, 485
Done, C. & Gierliński, M. 2006, MNRAS, 367, 659
Dove, J. B., et al. 1997, ApJ, 487, 759
Iaria, R., Gambino, A. F., Di Salvo, T., et al. 2018, MNRAS, 473, 3490
in 't Zand, J., Heise, J., Smith, M. J. S., et al. 1999, IAU Circ., 7138
Jain, C., et al. 2017, MNRAS, 468, L118
Kolehmainen, M., Done, C., & Díaz Trigo, M. 2011, MNRAS, 416, 311
Miller, L., Turner, T. J., Reeves, J. N., et al. 2007, A&A, 463, 131
Oosterbroek, T., et al. 2001, A&A, 376, 532
Reeves, J., Done, C., Pounds, K., et al. 2008, MNRAS, 385, L108
Sharma, R., Jaleel, A., Jain, C., et al. 2018, MNRAS, 481, 5560
Sidoli, L., et al. 2001, A&A, 379, 540
Wachter, S., Smale, A. P., & Bailyn, C. 2000, ApJ, 534, 367
Zdziarski, A. A., Johnson, W. N., & Magdziarz, P. 1996, MNRAS, 283, 193
Życki, P. T., Done, C., & Smith, D. A. 1999, MNRAS, 309, 561